

# A soft solid surface on Titan as revealed by the Huygens Surface Science Package

John C. Zarnecki<sup>1</sup>, Mark R. Leese<sup>1</sup>, Brijen Hathi<sup>1</sup>, Andrew J. Ball<sup>1</sup>, Axel Hagermann<sup>1</sup>, Martin C. Towner<sup>1</sup>, Ralph D. Lorenz<sup>2</sup>, J. Anthony M. McDonnell<sup>1</sup>, Simon F. Green<sup>1</sup>, Manish R. Patel<sup>1</sup>, Timothy J. Ringrose<sup>1</sup>, Philip D. Rosenberg<sup>1</sup>, Karl R. Atkinson<sup>1</sup>, Mark D. Paton<sup>1</sup>, Marek Banaszekiewicz<sup>3</sup>, Benton C. Clark<sup>4</sup>, Francesca Ferri<sup>5</sup>, Marcello Fulchignoni<sup>6</sup>, Nadeem A. L. Ghafoor<sup>7</sup>, Günter Kargl<sup>8</sup>, Håkan Svedhem<sup>9</sup>, John Delderfield<sup>10</sup>, Manuel Grande<sup>10</sup>, David J. Parker<sup>10</sup>, Peter G. Challenor<sup>11</sup> & John E. Geake<sup>12,‡</sup>

The surface of Saturn's largest satellite—Titan—is largely obscured by an optically thick atmospheric haze, and so its nature has been the subject of considerable speculation and discussion<sup>1</sup>. The Huygens probe entered Titan's atmosphere on 14 January 2005 and descended to the surface using a parachute system<sup>2</sup>. Here we report measurements made just above and on the surface of Titan by the Huygens Surface Science Package<sup>3,4</sup>. Acoustic sounding over the last 90 m above the surface reveals a relatively smooth, but not completely flat, surface surrounding the landing site. Penetrometry and accelerometry measurements during the probe impact event reveal that the surface was neither hard (like solid ice) nor very compressible (like a blanket of fluffy aerosol); rather, the Huygens probe landed on a relatively soft solid surface whose properties are analogous to wet clay, lightly packed snow and wet or dry sand. The probe settled gradually by a few millimetres after landing.

The Surface Science Package (SSP) comprises nine independent sensors. An in-depth technical description has been given in earlier papers<sup>3,4</sup>. The nine sensors were chosen such that some were designed primarily for landing on a solid surface and others for a liquid landing, with eight also operating during the descent. All sensors appear to have performed normally during the probe mission. Those sensors intended for a liquid landing scenario (refractometer, permittivity and density sensors) would have performed correctly for a liquid landing case; they are still under analysis for any secondary results. The SSP science data were redundantly transmitted on the two communication chains so that the loss of data on chain A did not result in any data loss for the SSP<sup>2</sup>.

The Acoustic Properties Instrument—Sonar (API-S) recorded the approach to the surface on final descent (Fig. 1). API-S is a pulse send—receive sonar, where the time of flight gives distance (and hence final descent speed). The probe vertical speed just before landing was determined as  $4.60 \pm 0.05 \text{ m s}^{-1}$ . The peak width and signal strength are influenced by surface topography, probe position and acoustic reflectivity according to the usual radar equation for an extended target.

As Huygens descended towards the surface the sensor footprint shrank, and a smaller area of terrain was illuminated. Owing to variation in probe tilt and wind drift during descent, the sensor illuminated different areas of ground for each pulse, with partial

overlap. Initial derivation of surface acoustic reflectivity shows no significant variation as a function of altitude, implying that the landing site as seen by Huygens is typical of the local surroundings (the maximum area sampled by API-S, for the highest altitude of around 90 m, is approximately a circle of 40 m diameter).

For all returns the peak widths are typically 30–50 ms wide, showing no trends. This implies that the surface is topographically

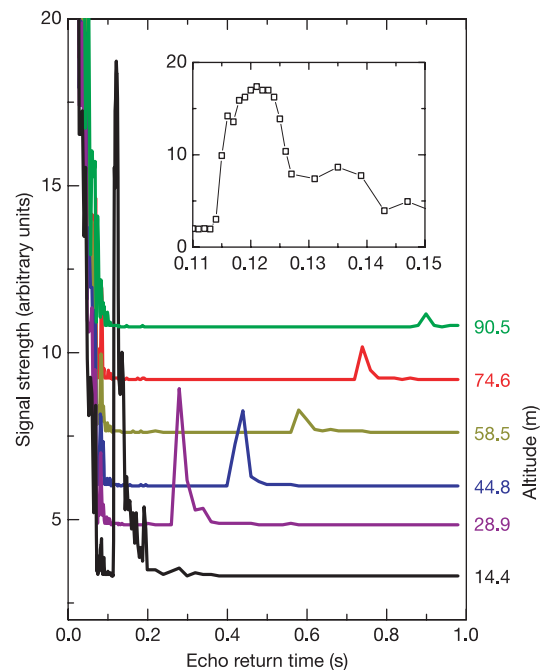


**Figure 1 | Acoustic sonar (API-S) surface echoes.** Note that the larger signals to the left of the plot are the result of the sensor ringing from the send pulse intruding into the receive time window. The inset is a zoom on the final API-S surface detection from 14.4 m altitude (at the time of pulse transmission). A speed of sound measurement of  $191.9 \pm 1.8 \text{ m s}^{-1}$  from the SSP Acoustic Velocity (API-V) sensors near the surface is used to convert ranging time delay into altitude.

<sup>1</sup>The Open University, Walton Hall, Milton Keynes MK7 6AA, UK. <sup>2</sup>University of Arizona, Lunar and Planetary Laboratory, Tucson, Arizona 85721, USA. <sup>3</sup>Polish Academy of Sciences, Ul Bartycka 18 A, Warszawa, PL-00716, Poland. <sup>4</sup>Lockheed Martin Astronautics, PO Box 179, Denver, Colorado 80201, USA. <sup>5</sup>CISAS G. Colombo, University of Padova, Via Venezia 15, 35131 Padova, Italy. <sup>6</sup>LESIA, Paris Observatory, 5 Place Janssen, 92195, Meudon, France. <sup>7</sup>MD Robotics, 9445 Airport Road, Brampton, Ontario, L6S 4J3, Canada. <sup>8</sup>Space Research Institute, Austrian Academy of Sciences, Schmiedlstraße 6, A-8042 Graz-Messendorf, Austria. <sup>9</sup>ESA/ESTEC, Research and Scientific Support Department, Postbus 299, 2200 AG, Noordwijk, The Netherlands. <sup>10</sup>Rutherford Appleton Laboratory, Chilton, Didcot, Oxon OX11 0QX, UK. <sup>11</sup>Southampton Oceanography Centre, Empress Dock, Southampton SO14 3ZH, UK. <sup>12</sup>Physics Department, UMIST, Manchester M60 1QD, UK.

‡Deceased.

similar over all sampled beam footprints. However, this width is greater than would be expected for a purely flat surface, implying that some small-scale vertical topography is present.

The final peak immediately before impact is at a height of 14.4 m at the time of pulse transmission, with a beam footprint of  $\sim 26 \text{ m}^2$  (equivalent to a circle of  $\sim 2.9 \text{ m}$  radius). This final peak is recorded by the SSP at higher time resolution than previous ones, giving more information on surface structure (Fig. 1 inset). The relatively broad shape of this peak indicates that the surface cannot be completely flat, or concave over the footprint. However, the flat top of the peak also requires that there be some local height variation over the surface sampled within the footprint. Rock size determined from the post-landing surface images will provide a good starting point for further collaborative analysis. When averaged to a lower time resolution, the width of the final peak is entirely comparable to the width of the higher-altitude peaks, implying that they are seeing very similar terrain.

Together these data suggest a surface that is relatively flat but not completely smooth; such an interpretation is compatible with the Descent Imager and Spectral Radiometer (DISR) surface images, suggesting that perhaps the DISR images show a typical surface that probably surrounds the probe in all directions. The fact that slight horizontal and vertical topographic variation is seen over the footprints, rather than a completely flat plain, implies a certain level of complexity during the history of surface formation in the region of the landing site.

There is a well-established history of determining the mechanical properties of a planetary surface from the dynamics of a spacecraft landing<sup>5</sup>. Titan's outer surface layers were expected to be dominated by water ice and organic materials, although other ices and minerals could not be ruled out. As with other planetary surfaces, these materials might be processed by impacts, volcanism and erosion<sup>1</sup>. The SSP includes an impact penetrometer and an accelerometer to measure mechanical properties of the surface material at the landing site. The ACC-I accelerometer is a single-axis piezoelectric accelerometer able to produce a successful measurement for all survivable landing scenarios, but for the hardest surfaces it was more likely that the structures of the probe would have been crushed, damping the measured deceleration. For such cases the impact penetrometer (ACC-E) was provided to measure directly the penetration resistance of the ground<sup>5,6</sup>, yielding strength and texture information through a piezoelectric force transducer positioned behind a 16-mm-diameter hemispherical tip.

ACC-I and ACC-E together covered the wide range of properties that could have been encountered, from liquids or very soft material to solid, hard ice. Their ranges of applicability overlapped—for intermediate-strength materials the surface would be soft enough not to crush the probe, and thus produce meaningful output from the accelerometer, yet hard enough also to produce a meaningful signal from the penetrometer. Also measuring the impact dynamics were SSP's two-axis tilt sensor (TIL) and the three piezoresistive (PZR) accelerometers of the Huygens Atmospheric Structure Instrument Accelerometer (HASI ACC) experiment subsystem<sup>7</sup>.

Figure 2 shows the impact signatures from the penetrometer and accelerometers. The impact triggered ACC-E at a mission time<sup>2</sup> of  $T_0 + 8,869.7598 \text{ s}$  as the penetrometer tip penetrated the surface, followed by ACC-I, which triggered at  $T_0 + 8,869.7695 \text{ s}$  as the probe foredome struck the surface ( $T_0$  is defined as the start of the descent sequence at 09:10:21 UTC). This event also seems to have caused the broad peak in the ACC-E signal following the period of 'clean' penetration. The observations that ACC-E triggered with a signal containing detailed structure and ACC-I returned a signal of brief duration with minimal rebound immediately ruled out a liquid landing.

The raw signal from ACC-E has been processed to correct for the transfer function of the electronics and digitization noise at the analog-to-digital converter (ADC). The processed, calibrated signal

(Fig. 3) shows the following features: a shallow rise at the start of the event; a strong peak; a smooth plateau at around 50 N, and a broad, smooth peak once the measurement is disrupted by impact of the probe's foredome. The near-constant force of 50 N over its  $\sim 2 \text{ cm}^2$  projected area gives a dynamic penetration resistance of 250 kPa. Terrestrial materials with these strength characteristics include lightly packed snow, tar, and wet sand or clay. Initial results from laboratory experiments using an identical penetrometer striking at  $3.7 \text{ m s}^{-1}$  (the maximum velocity currently achievable with our test rig) into a range of room-temperature analogue targets suggest that the signal is consistent with an ACC-E impact into a moderately firm, perhaps wet granular material overlain by an ice pebble or—perhaps less likely, given the prevalence of pebbles and cobbles in the DISR surface images<sup>8</sup>—a thin crust, and in either case coated with a very soft top layer. The signal's subsurface plateau phase shows a lack of prominent positive-going short-period structure, yet is not completely smooth, indicating the presence of some small-scale texture. This is consistent with the penetrometer encountering a mixture that is likely to be poorly sorted but containing nothing coarser than sand, granules and small pebbles (as defined by the Udden–Wentworth scale<sup>9</sup>). Some inhomogeneity, including voids, may also be present. The slight downward trend in the plateau phase could be consistent with the presence of liquid among the grains and a liquid content increasing with depth.

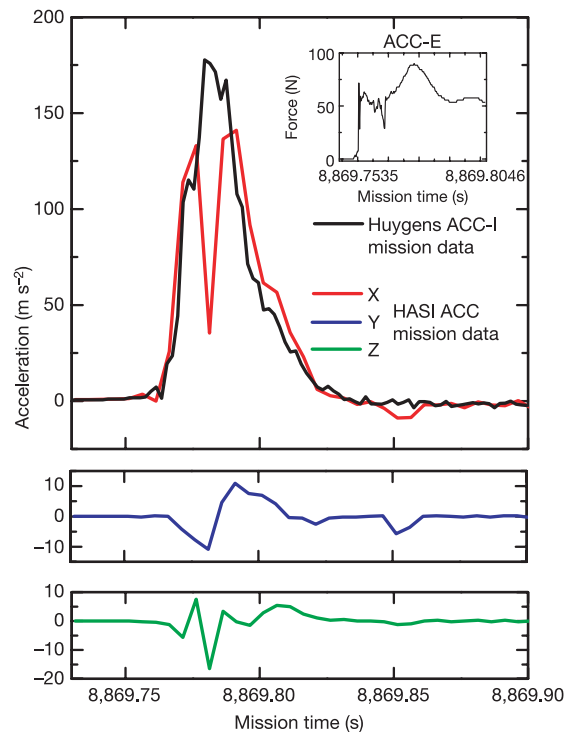


**Figure 2 | Impact deceleration profiles.** Main panels, SSP ACC-I (black) and HASI ACC PZR X, Y, Z (red, blue, green) accelerometer impact signatures, with SSP ACC-E penetrometer impact signature (inset). ACC-I (a single-axis piezoelectric accelerometer) and PZR X (a piezoresistive accelerometer) are both aligned parallel to the probe's axis, while PZR Y, Z are perpendicular, to measure transverse accelerations. Note that the PZR data has been time-shifted to match the ACC-I impact time; this is within the 125 ms uncertainty between the two experiments. The ACC-I accelerometer (an Endevco 2271 AM20) is aligned with the probe's axis of symmetry (X axis) but mounted 0.325 m from it, on the SSP electronics box. It was sampled at 500 Hz with 12 bit resolution over the range  $\pm 90g$  for a duration of 512 samples. The HASI PZR sensors (Endevco type 7264A-2000T) were mounted close to the probe's centre of mass. They had an absolute accuracy of  $\pm 4 \text{ m s}^{-2}$  and resolution of  $0.15 \text{ m s}^{-2}$ , and were sampled at 200 Hz.

Both ACC-I and the (parallel) HASI ACC PZR X sensor (see Fig. 2 legend for definitions of PZR X, Y and Z) registered a small precursor peak of a few  $\text{m s}^{-2}$  in amplitude. Although it is tempting to associate this with the impact of the ACC-E penetrometer, the peak is an order of magnitude larger than would be obtained from the peak force actually measured by ACC-E. One possibility is that it may be due to impact of the probe's foredome with an isolated protuberance such as an 'ice cobble' resting on the surface.

The peak decelerations parallel to the probe's axis seen by ACC-I and PZR X were  $178 \text{ m s}^{-2}$  and  $141 \text{ m s}^{-2}$ , respectively. The cause of the double peak structure of the PZR X signal is currently under investigation; it might be due to a high-frequency resonance of the experiment platform being sampled by the HASI electronics at a lower frequency of 200 Hz, rather than real probe dynamics. ACC-I showed little if any such dip—if platform resonance were responsible for the dip, then this could be explained by the location of ACC-I closer to the vibrational node around the platform's edge. After initial transfer function processing and integration, the ACC-I signal gives a speed change of  $4.63 \text{ m s}^{-1}$  with minimal bounce. This is corroborated by the PZR X data, which give a peak of  $4.33 \text{ m s}^{-1}$ . Further integration of the accelerometry leads to an estimate of the distance over which the probe decelerated of 0.12 m. The radius of curvature of the probe foredome is 1.215 m, thus the maximum contact area (assuming a 0.12 m penetration) is  $0.92 \text{ m}^2$ . The deceleration peaks at a distance of 0.09 m, at which point the maximum contact area would be approximately  $0.69 \text{ m}^2$ . A deceleration of the 200.5 kg probe of  $178 \text{ m s}^{-2}$  requires a force of 36 kN. Exerted over the contact area indicated above, this implies a dynamic penetration resistance of  $> \sim 52 \text{ kPa}$ . This is a tighter constraint than that implied by the

persistence of  $\sim 0.1\text{-m}$ -scale cobbles (in DISR surface images<sup>8</sup>), supported by the bulk surface material which implies bearing strength of  $> \sim 0.1 \text{ kPa}$ . The magnitudes of these accelerations also rule out the presence of a very hard consolidated material down to the depth penetrated.

The difference between the penetrometer and accelerometer determinations may indicate some structural filtering by the probe, or that the penetrometer may have struck a site harder than the average beneath the probe. Such a discrepancy may not be surprising, given the presence of the  $\sim 0.1\text{-m}$ -scale cobbles. The accelerometer and penetrometer results may be reconciled if the probe, instead of landing directly on the 250-kPa-strength substrate sampled by the penetrometer, crashed onto ice cobbles with a collective area of  $\sim 0.2 \text{ m}^2$ . These cobbles in turn pushed into the substrate, acting as 'penetrometers' themselves with a smaller area than the foredome, and thus yielding the modest observed deceleration.

Preliminary evaluation by comparison with scale models<sup>10</sup> and numerical simulations<sup>11</sup> suggests that the surface was neither hard (like solid ice) nor very compressible (like a blanket of fluffy aerosol). Analogue materials with mechanical properties consistent with the data include tarry materials like wet clay, somewhat cohesive material like lightly packed snow, and wet or dry sand. Interpretation is complicated by the possible presence of cobbles resting on the surface (DISR), which would change the effective shape of the penetrating probe (from the case of a flat surface).

The probe's apparent tilt (that is, the angle between the probe's axis and the tiltmeter's instantaneous acceleration vector) just before landing was around  $9^\circ$ , but had been varying in the range  $4\text{--}16^\circ$  during the 20 s before impact, on timescales at least as short as the 1 s sampling interval. By averaging the signal over the final 1 km of descent to smooth out the dynamic effects of probe motion, it is clear that there existed a mean tilt of about  $8^\circ$ . Oscillations are visible in the TIL signal until some 10 s after landing. Damped oscillations within the TIL sensors may offer only a partial explanation for this, suggesting that the probe took several seconds to come to a final rest. The probe's tilt after the impact event was very similar to that before impact, at  $10.3^\circ$ . This suggests that the surface material was deformed largely plastically (whether by shear or brittle failure and compression) and was readily penetrated.

TIL indicates a gradual change in the angle of the probe at a rate of  $0.2^\circ \text{ h}^{-1}$  during the 70 min after landing for which data were received. This is corroborated by data from the HASI ACC X servo-accelerometer (the high resolution part of the HASI ACC experiment subsystem, co-aligned with the PZR X sensor), which shows a similar rate of change. The HASI data would give the same absolute magnitude of tilt as that from TIL if one assumed the value of gravity at a radius of  $2,578.5 \pm 1 \text{ km}$ , as compared with the published value<sup>2</sup> of  $2,575 \pm 2 \text{ km}$ , which gives an apparent tilt difference of  $< 0.5^\circ$ . This is tentative, however, as measurements are taken at the limit of resolution of the sensors. This degree of settling amounts to a shift of a few millimetres in the probe's position.

Modelling<sup>1</sup>, together with optical, radar and infrared spectrometer images from Cassini<sup>12–14</sup> and images from the Huygens probe<sup>8</sup> indicate a variety of possible processes modifying Titan's surface. These include tectonism, cryovolcanism, impacts and fluvial erosion. Fluvial and marine/lacustrine processes appear most prominent at the Huygens landing site, although aeolian activity cannot be excluded. Thus the SSP and HASI accelerometer impact dynamics data are consistent with two plausible interpretations for the soft substrate material: solid, granular material having either low or zero cohesion, or a fluid component. The mixture resulting from the latter possibility would be analogous to a wet sand or a textured tar/wet clay. These possibilities, between which our data alone cannot discriminate, would involve 'sand' made presumably of ice grains from impact or fluvial erosion, wetted by liquid methane, or a collection of photochemical products and/or fine-grained ice making a plastic or viscoplastic material, that is, a 'tar'.

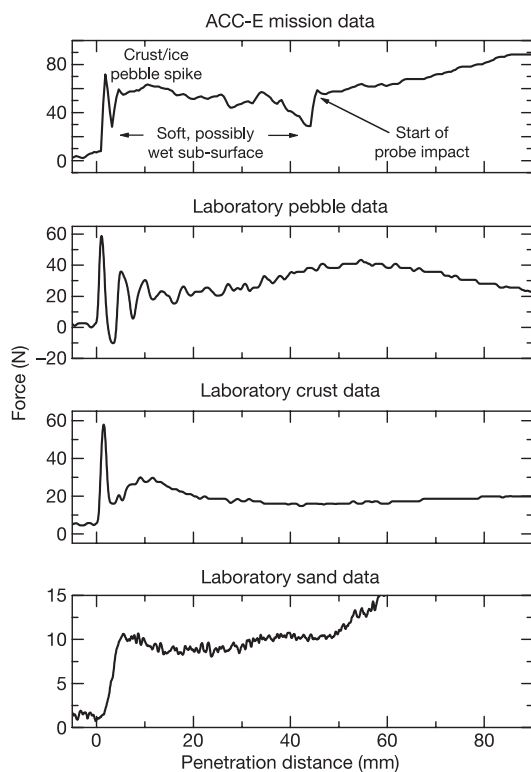


**Figure 3 | A comparison of penetrometer force profiles for Titan and laboratory analogues.** Top to bottom: SSP ACC-E mission data, and laboratory data for impact onto a pebble, impact onto a surface crust layer, and impact onto sand. ACC-E was mounted on a pylon that protruded below the probe foredome to give 55 mm of undisturbed penetration before the main structure of the probe contacted the surface. The force measurement employed pseudo-logarithmic amplification and was sampled at 10 kHz and 8 bit resolution with a range of approximately 6 kN (although structural failure would occur at around 2 kN) for a duration of 512 samples.

Received 2 June; accepted 6 September 2005.

Published online 30 November 2005.

1. Lorenz, R. D. & Lunine, J. I. Titan's surface before Cassini. *Planet. Space Sci.* **53**, 557–576 (2005).
2. Lebreton, J.-P. *et al.* An overview of the descent and landing of the Huygens probe on Titan. *Nature* doi:10.1038/nature04347 (this issue).
3. Zarnecki, J. C. *et al.* in *Huygens: Science, Payload and Mission* (ed. Wilson, A.) 177–195 (SP-1177, ESA Publications Division, Noordwijk, The Netherlands, 1997).
4. Zarnecki, J. C., Leese, M. R., Garry, J. R. C., Ghafoor, N. & Hathi, B. Huygens' Surface Science Package. *Space Sci. Rev.* **104**, 593–611 (2002).
5. Kömle, N. I., Kargl, G., Ball, A. J. & Lorenz, R. D. (eds) *Penetrometry in the Solar System* (Austrian Academy of Sciences Press, Vienna, 2001).
6. Lorenz, R. D. *et al.* An impact penetrometer for a landing spacecraft. *Meas. Sci. Technol.* **5**, 1033–1041 (1994).
7. Fulchignoni, M. *et al.* *In situ* measurements of the physical characteristics of Titan's atmosphere. *Nature* doi:10.1038/nature04314 (this issue).
8. Tomasko, M. *et al.* Rain, winds and haze during the Huygens probe's descent to Titan's surface. *Nature* doi:10.1038/nature04126 (this issue).
9. Wentworth, C. K. A scale of grade and classification terms for clastic sediments. *J. Geol.* **30**, 377–392 (1922).
10. Seiff, A. *et al.* Determination of physical properties of a planetary surface by measuring the deceleration of a probe upon impact: Application to Titan. *Planet. Space Sci.* **53**, 594–600 (2005).
11. Lorenz, R. D. Huygens probe impact dynamics. *ESA J.* **18**, 93–117 (1994).
12. Porco, C. C. *et al.* Imaging of Titan from the Cassini spacecraft. *Nature* **434**, 159–168 (2005).
13. Elachi, C. *et al.* Cassini radar views the surface of Titan. *Science* **308**, 970–974 (2005).
14. Sotin, C. *et al.* Release of volatiles from a possible cryovolcano from near-infrared imaging of Titan. *Nature* **435**, 786–789 (2005).

**Acknowledgements** We acknowledge the work of the SSP Team and the HASI Accelerometer Team both past and present in the design, build, test, calibration and operation of these experiments. This work has been funded by the UK Particle Physics and Astronomy Research Council, The Royal Society, the ESA, NASA, CNES and the Polish State Committee for Scientific Research.

**Author Information** Reprints and permissions information is available at [npg.nature.com/reprintsandpermissions](http://npg.nature.com/reprintsandpermissions). The authors declare no competing financial interests. Correspondence and requests for materials should be addressed to J.C.Z. (J.C.Zarnecki@open.ac.uk).